Available at www.ComputerScienceWeb.com
POWERED BY SCIENCE DIRECT®

Pattern Recognition Letters 24 (2003) 705–713

Pattern Recognition Letters

www.elsevier.com/locate/patrec

Decompression and speckle detection for ultrasound images using the homodyned *k*-distribution

R.W. Prager [a,*], A.H. Gee [a], G.M. Treece [a], L.H. Berman [b]

[a] *Department of Engineering, University of Cambridge, Trumpington Street, Cambridge CB2 1PZ, UK*
[b] *Department of Radiology, University of Cambridge, Level 5, Box 219, Addenbrooke's Hospital, Hills Road, Cambridge CB2 2QQ, UK*

Abstract

The ultrasound envelope intensity distribution can be used for speckle detection and for measuring the distance between images by speckle decorrelation. However, this intensity signal is rarely available. Many researchers work with B-scan data which has been scan-converted and subject to nonlinear mappings to compress the dynamic range. This paper presents an approximate algorithm for recovering the intensity signal from B-scan data. It is then used as the basis of a speckle detector using the statistics of a homodyned *k*-distribution.

Keywords: Ultrasound; Speckle detection; Logarithmic compression; *k*-Distribution

1. Introduction

There is a considerable body of theory associated with the ultrasound envelope intensity distribution. Raw data in this form can be used for speckle detection (Dutt and Greenleaf, 1994), to govern adaptive speckle suppression algorithms (Dutt and Greenleaf, 1996a) and for measuring the distance between images by speckle decorrelation (Li, 1995; Chen et al., 1997; Tuthill et al., 1998).

However, ultrasound data is most easily available in the form of a B-scan, after it has been subject to scan conversion (resampling onto a rectangular grid), logarithmic compression and other proprietary nonlinear mappings built into the ultrasound machine. These processes affect the statistics of the data and many of the attractive properties theoretically derived for the raw intensity data are lost.

In this paper, we present an iterative strategy for deriving the approximate envelope intensity signal from the pixel values of a displayed B-scan. We then describe an extension of the algorithm of Dutt and Greenleaf (1994) which uses this information to detect the regions of speckle in the image. The intensity speckle signal, generated from conventional B-scans by these techniques, has the correct statistical properties to be used in decorrelation algorithms (Chen et al., 1997), thus enabling the acquisition of 3D ultrasound without requiring either a position sensor, or access to low level signals from within the ultrasound machine.

* Corresponding author.
E-mail address: rwp@eng.cam.ac.uk (R.W. Prager).

0167-8655/03/$ - see front matter
PII: S0167-8655(02)00176-9

2. Finding the envelope intensity from the B-scan pixel value

To compute the intensity signal, we need to invert the logarithmic compression and other nonlinear signal processing performed by the ultrasound machine. Several groups of researchers (Crawford et al., 1993; Kaplan and Ma, 1994; Dutt and Greenleaf, 1996b; Smith and Fenster, 2000) suggest a mapping of the form $p = D\ln(I) + G$, where p is the B-scan pixel value, I is the envelope intensity, and D and G are parameters of the mapping. Crawford et al. (1993) report that provided the parameters of the mapping are chosen correctly, it can be used to approximately invert the compression algorithms employed by a number of different ultrasound machine manufacturers.

The parameter G does not affect many of the statistics used to measure speckle, such as the mean divided by the standard deviation, the normalised moments or the skewness of the distribution. Furthermore, it does not affect the normalised autocovariance used in the decorrelation algorithms for elevational distance measurement, provided the same G values are used in the two images being compared (Chen et al., 1997). This is likely to be a reasonable assumption if G does not change rapidly across the image.

The challenge, therefore, is to determine an appropriate value for D. Crawford et al. (1993) use measurements based on a calibrated phantom, while Kaplan and Ma (1994) require access to the data before scan conversion, which is not often possible with commercially available ultrasound machines.

In this section we present an iterative approach to determining the compression factor D directly from a speckled patch in the ultrasound image. In Section 3, we show that this approach is more robust to the nonlinear mappings built into ultrasound machines than the formula of Kaplan and Ma.

Fully developed speckle is generated when a large number of weak scatterers of random phase contribute to the signal from each resolution cell of the ultrasound image. The intensity values of this signal are known to approximately follow an exponential distribution (Wagner et al., 1983). Our approach is to match the measured normalised moments of I in known speckle regions with the expected values for an exponential distribution. The value of D can thus be found from a small number of manually selected speckle patches, and then used to determine intensity values for any images obtained using the same ultrasound machine configuration.

In Appendix A we show that the normalised moments, $\langle I^n\rangle/\langle I\rangle^n$, of the exponential distribution are given by $\Gamma(n+1)$. This is true for positive values of n which are not necessarily integers. The algorithm proceeds as follows:

(1) Choose an initial value for D. (We use 30; the algorithm is not particularly sensitive to the starting value.)
(2) Invert the compression mapping for a patch of known speckle using intensity = exp(Pixel value/D).
(3) Compute the normalised moments of the intensity data for the powers $n = 0.25$, 0.5, 1.5, 2.0, 2.5 and 3.
(4) Calculate an error vector from the differences between the six normalised moments computed and the normalised moments of an exponential distribution.
(5) If the sum squared magnitude of the error vector is small compared to the machine precision, or the search has converged to a (potentially local) minimum of this error function: finish.
(6) Use an optimisation algorithm (e.g. Levenberg Marquart) to estimate a value of D that reduces the sum squared magnitude of the error vector. Continue from step 2.

For ease of reference, we call this the fractional moments algorithm for extraction of decompression parameters. To test the algorithm, 50 sets of 3249 [1] random numbers were generated with an

[1] There is no particular significance in the number $3249 = 57^2$. For low noise in the statistics we want large samples, but smaller samples enable more fine-grained analysis. For this work, a sample size between 3000 and 4000 provides a sensible compromise.

Table 1
Results of sets of 50 simulations to estimate the decompression factor D using samples from an exponential distribution

	Mean of errors in D (i.e. bias)	Standard deviation of errors
32490 numbers un-rounded	+0.006	0.10
32490 numbers rounded	+0.013	0.11
3249 numbers un-rounded	−0.039	0.33
3249 numbers rounded	−0.034	0.33

Two sample sizes were used and in each case the algorithm was run on the compressed data both before and after rounding to integers.

exponential probability density function (PDF). They were then compressed using values of $D =$ 12, 13, 14 and 15. A constant offset, G, was added to each set of compressed data to make the numbers lie in the range 0–255. Fifty larger sets were similarly generated, each containing 32,490 numbers.

The iterative algorithm was applied to all the data, both directly to the real numbers produced by the logarithmic compression, and after these numbers had been rounded to integers. An analysis of the errors is given in the Table 1.

These results show that the fractional moments algorithm appears to be effective in estimating D in simulation. There is an advantage in using a large block of fully developed speckle but the rounding process in the logarithmic compression does not significantly affect the performance.

3. Detecting speckle in the intensity image

In this section, we build a parametric model of the statistics of ultrasound images and select as speckle those parts of an image that correspond to parameters close to the theoretical values for fully developed speckle.

Fully developed speckle is generated by a large number of scatterers with random phase in each resolution cell. When there are fewer random scatterers in each cell we get partially developed speckle. Clifford et al. (1993) and Weng et al. (1991) have demonstrated that the k-distribution, with parameter μ equal to the effective number of scatterers in each resolution cell, is a good model for the amplitude distribution of the received signal in this case. Various researchers have estimated speckle parameters based on its moments (Dutt and Greenleaf, 1995; Ossant et al., 1998).

When the phase of the reflectors in each cell is not random, we get coherent scattering, often leading to clear bright features in the B-scan images. For this case Jakeman and Tough (1987) suggest that the homodyned k-distribution provides a better model than the generalised k-distribution, based on its performance when the proportion of diffuse scattering is low relative to the amount of coherent reflection. The homodyned k-distribution has two further parameters (in addition to μ), that specify the coherent signal energy s^2, and the diffuse, (i.e. random phase), signal energy $2\sigma^2$ (see Appendix B).

Dutt and Greenleaf (1994) use an iterative approach to finding parameters of an underlying homodyned k-distribution from patches of an image. In this section, we present an analytical solution to this problem and use it to demonstrate the robustness of the fractional moments algorithm, presented in the previous section, in the presence of a nonlinear mapping from an ultrasound machine.

Following the approach of Dutt and Greenleaf, we wish to extract the following two derived parameters from a patch of image data: $k = s/\sigma$ and $\beta = 1/\mu$. The moments of the distribution of the intensity data can be expressed in terms of these parameters: the amplitude is homodyned k-distributed and the intensity, I, is obtained by squaring it.

$$\langle I \rangle = \sigma^2[k^2 + 2]$$

$$\langle I^2 \rangle = \sigma^4[8(1+\beta) + 8k^2 + k^4]$$

$$\langle I^3 \rangle = \sigma^6[48(1 + 3\beta + 2\beta^2) + 72k^2(1+\beta) + 18k^4 + k^6]$$

Using these expressions, we can compute two statistics: R, the ratio of the mean to the standard deviation, and S, the skewness.

$$R = \frac{\text{mean}}{\text{standard deviation}} = \frac{\langle I \rangle}{\sqrt{\langle I^2 \rangle - \langle I \rangle^2}} = \frac{k^2 + 2}{2\sqrt{k^2 + 2\beta + 1}} \quad (1)$$

$$S = \text{skewness} = \frac{\langle (I - \langle I \rangle)^3 \rangle}{(\langle I^2 \rangle - \langle I \rangle^2)^{3/2}} = \frac{(k^2 + 2\beta + 1)(6\beta + 3) - 1}{(k^2 + 2\beta + 1)^{3/2}} \quad (2)$$

Notice that σ has cancelled out of the equations leaving R and S in terms of just k and β. Adding together $6R + S$, we get a quartic equation $3U^4 - (6R + S)U^3 + 6U^2 - 1 = 0$ in $U = \sqrt{k^2 + 2\beta + 1}$, which is solved in Appendix C. Useful positive solutions for k and β only exist for certain values of R and S. The solution domain is found by solving for the lines $k = 0$ and $\beta = 0$ in R–S space. These are shown in Fig. 1. Positive real solutions for k and β only exist above the solid line $k = 0$ and the dashed line $\beta = 0$.

Two sets of simulations were performed, each with 120 sets of 3249 random samples from homodyned k-distributions with various parameters, as follows: $\sigma = 1$; $s = 1$, 2, 3, 4, 5, 6, 7, 8, 9 and 10; $\mu = 1$, 2, 3, 4, 5, 6, 7, 8, 9, 10, 11 and 12. These resulted in a range of values for the derived parameters $k = s/\sigma$ and $\beta = 1/\mu$.

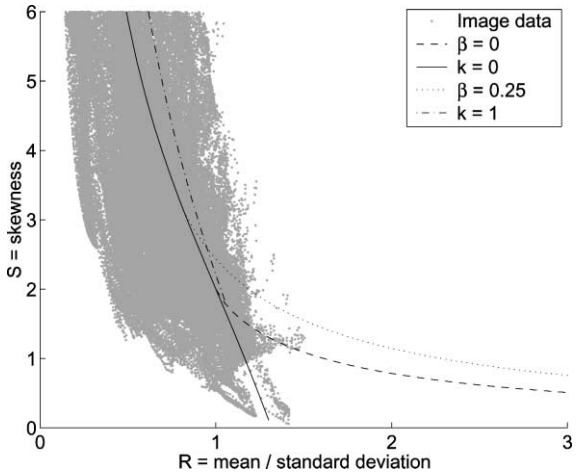

Fig. 1. Graph of S = skewness against R = mean/standard deviation. The (R, S) values of patches analysed in an uncompressed ultrasound image are shown shaded. Lines are plotted for $k = 0$, $k = 1$, $\beta = 0$ and $\beta = 1/4$. Positive real solutions for k and β only exist above the lines $k = 0$ and $\beta = 0$.

The first set of simulations involve only logarithmic compression of the intensity signal.

(1) 3249 random numbers are generated from an approximately homodyned k-distribution [2] with the required k and β. These numbers are then squared to form an intensity signal.
(2) The data is logarithmically compressed and rounded to integers in the range 0–255.
(3) 3249 samples from a squared Rayleigh (i.e. exponential) distribution are compressed using the same compression parameters.
(4) The D parameter of the logarithmic compression is estimated from the compressed Rayleigh data using the algorithm described in Section 2 above and also using equation (8) of Kaplan and Ma (1994) (adapted to map to intensity rather than amplitude), $D = \sqrt{6v/\pi}$, where v is the variance of the log-compressed data.
(5) The compressed data from the homodyned k-distribution is uncompressed using each of the parameter estimates from step 4, and the statistics R and S are calculated in each case.
(6) k and β are found from each pair of R and S values using the method described above.

A second set of simulations was then performed to assess the robustness of the two approaches when the data is subject to an additional nonlinear mapping. To do this, the procedure above was repeated with a nonlinear mapping applied to both the homodyned k, and Rayleigh, data at the end of steps (2) and (3). The mapping was the default pixel transformation used by a commercially available ultrasound machine, [3] and is shown in Fig. 2.

While the algorithm described in Section 2 is able to partially compensate for a nonlinear mapping, a further correction to the measured

[2] The random data is generated using the inverse method (Abramowitz and Stegun, 1970, p. 950) to create k-distributed data, before adding the coherent component of amplitude s.

[3] The approximate shape of the mapping is given by $y = 14(\exp(-x/73.6) - 1) + 272(\exp(x/396.7) - 1)$.

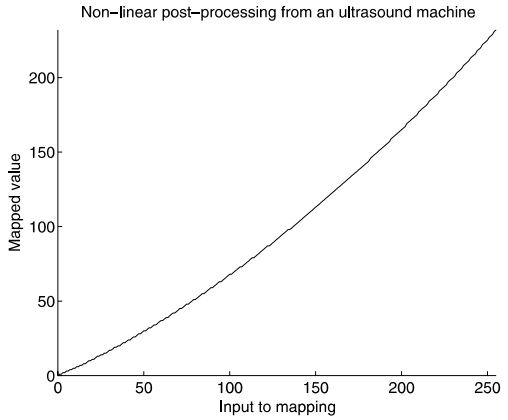

Fig. 2. One of the post-processing mappings used by the Diasus ultrasound machine produced by Dynamic Imaging Ltd.

values of R and S can be used to improve the resulting estimates of k and β. Once the iterative procedure for finding the decompression factor D has converged, the values of R and S from the idealised speckled data are compared with theoretical predictions for fully developed speckle ($R = 1$, $S = 2$). The errors observed are used as additive corrections to the values of R and S calculated from the uncompressed homodyned k data before solving for k and β. This correction is valid for R and S values close to those for speckle and thus improves estimates of k and β when they are both small.

The results are shown in Fig. 3. Graph (a) shows that both decompression algorithms work well for the idealised data. The mean squared

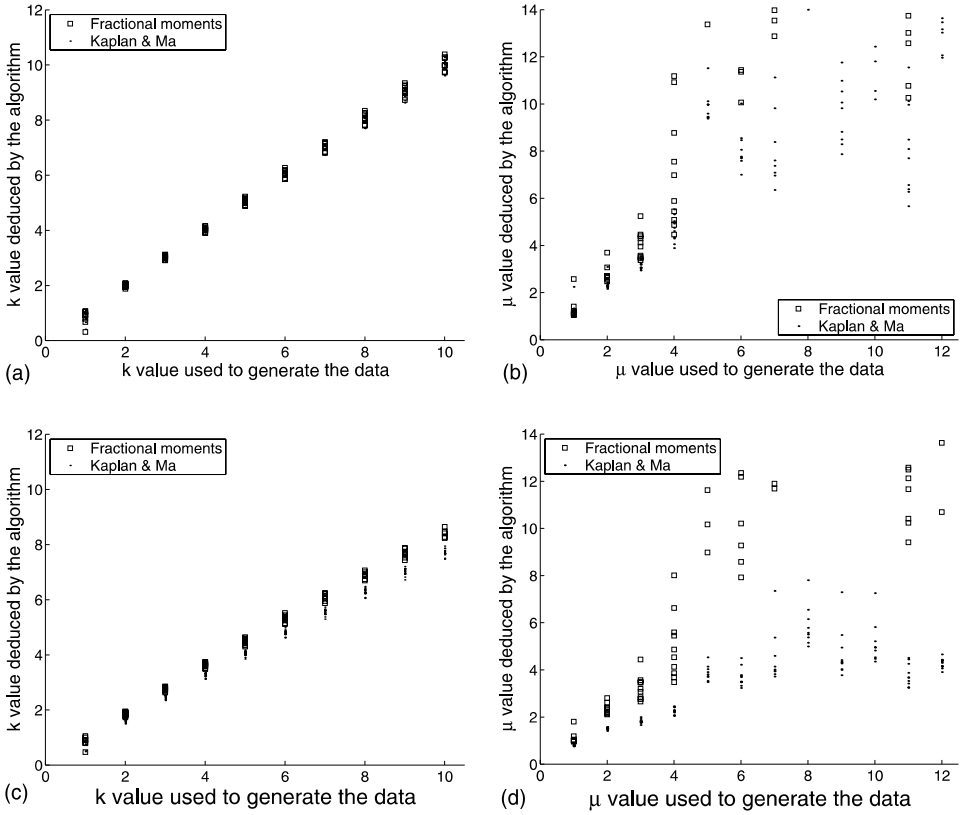

Fig. 3. k and μ values extracted from compressed simulated data. In (a) and (b) the data is just logarithmically compressed. In (c) and (d) a nonlinear mapping from an ultrasound machine post-processor is also applied. Graph (c) shows that the fractional moments algorithm is more robust than Kaplan and Ma's algorithm and partially compensates for the nonlinear mapping.

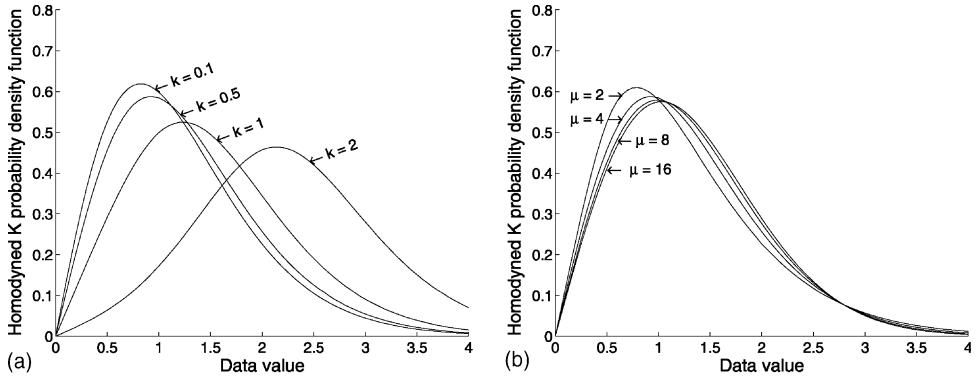

Fig. 4. Graph (a) shows the homodyned k PDF for $\sigma = 1$, $\mu = 4$ and various values of s, resulting in corresponding (equal) values of k. Graph (b) shows the same density function for $\sigma = 1$, $s = k = 0.5$ and various values of μ. Notice that the graph shape changes more with variation in k than it does for variation in μ.

error in k for the fractional moments approach is 0.023 and for Kaplan and Ma's approach is 0.021. The standard error for these figures is about 0.004. Graph (c) shows that the fractional moments algorithm is more robust and partially compensates for the nonlinear mapping, resulting in a mean squared error of 0.606 (standard error 0.074) compared to a figure for the Kaplan and Ma approach of 1.861 (standard error 0.162).

Graphs 3(b) and (d) show similar results for estimating μ. The deduced value of μ is unreliable above about 4 for the sample size used in the experiment (3249). The reason for this can be seen from the graphs of PDFs shown in Fig. 4. There is much less variation in the graph shape for different values of μ than there is for different k.

4. Experiments on B-scan data

The decompression and speckle identification algorithms were run on ultrasound data of a liver and kidney in order to illustrate their operation. Two square (57×57 pixel) patches of fully developed speckle were manually identified in one of the scan images. These are shown in Fig. 5(a). The algorithm of Section 2 was applied to the speckle pixel values from these squares (and similar data from nine neighbouring images) and an estimate of the effective logarithmic compression factor, D, was obtained.

Decompression factor	$D = 19.08$	
Mean/standard deviation	$R = 1.07$	(should be 1 for fully developed speckle)
Skewness	$S = 2.95$	(should be 2 for fully developed speckle)

Using these results, the complete images were decompressed to give an effective intensity signal, $I = \exp(p/D)$, from the pixel value, p, in the B-scan. The algorithm from Section 3 was then used to identify regions of speckle in the images. Round patches of 3249 pixels (radius 32.2 pixels) were analysed at every point in each image and two statistics, $R =$ mean/standard deviation and $S =$ skewness, were computed. These figures were then corrected using the residual errors observed during the calculation of the decompression parameter, by subtracting 0.07 from R and 0.95 from S. The resulting cloud of points in (R, S) space is shown as shading in Fig. 1.

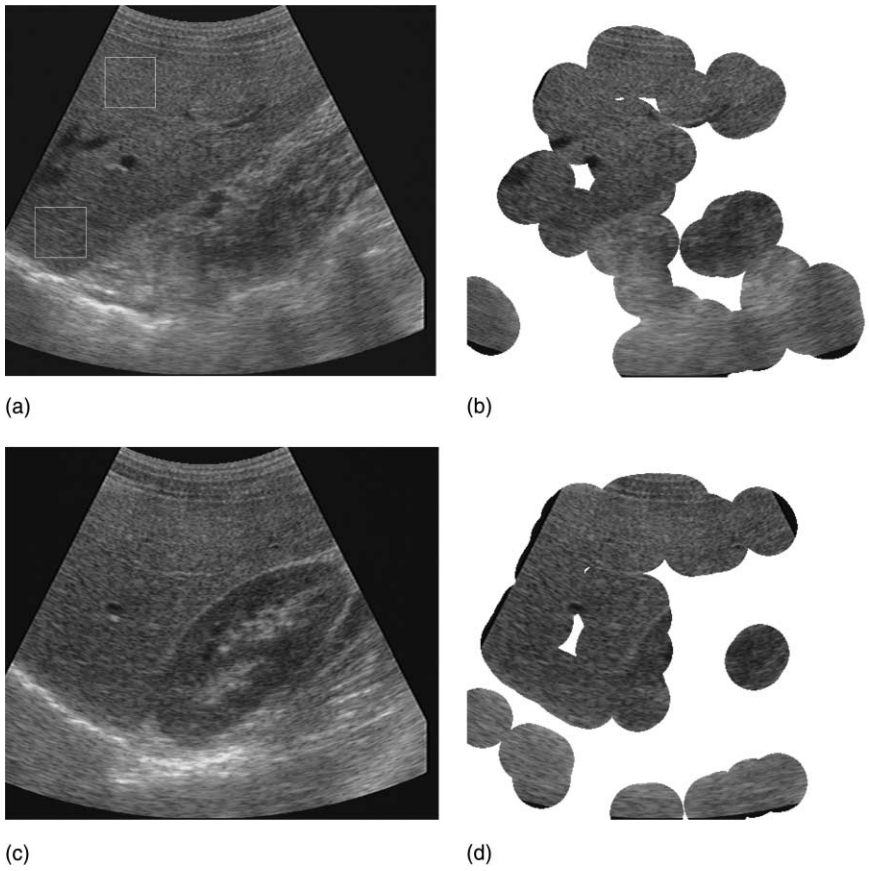

Fig. 5. Results: (a) first frame of a scan through a liver and kidney, showing the manually identified speckle regions (in the liver) used to determine the image decompression parameters, (b) speckle found in the image shown in (a), (c) 162nd frame of a scan through a liver and kidney and (d) speckle found in the image shown in (c).

To identify speckle in the images we require thresholds for k and β. With samples of size 3249, we know from the experiments in Section 3 that estimates of μ above 4 are unreliable, so we cannot expect to differentiate between values of β below $1/4$. We therefore set our β threshold at $1/4$. We choose a threshold of 1 for k, so as to accept any patch in which the intensity of diffuse speckled reflection is greater than the intensity of coherent reflection. The borders defined by these thresholds in R–S space are shown in Fig. 1. The sliver of space between them is the region deemed to contain points with statistics derived from predominantly speckled data.

Where an image patch has statistics that meet the rules $0 \leqslant k < 1$, and $0 \leqslant \beta < 1/4$ all the points in the patch are accepted as speckle. The speckle found in the first frame of the data set is shown in Fig. 5(b). Fig. 5(c) shows the 162nd frame of the data and Fig. 5(d) shows the speckle regions identified in it.

5. Discussion and conclusions

We have presented the fractional moments algorithm for the decompression of B-scan ultrasound images to produce an approximate intensity signal. This algorithm produces similar results to the quicker approach of Kaplan and Ma (1994) for pure logarithmic compression, but also works in

the presence of a nonlinear mapping where the Kaplan formula does not apply.

The envelope intensity obtained from the decompression process can be used by a variety of algorithms that rely on the statistics of the ultrasound signal. These include speckle detection algorithms, adaptive speckle suppression algorithms, and algorithms for measuring the distance between B-scan slices using speckle decorrelation.

We have also presented an extension of the approach of Dutt and Greenleaf (1994) to perform speckle identification in B-scan images. We have described a new analytical means of solving for the parameters of the underlying homodyned k-distribution from statistics of the data. This has been tested on simulated data to produce quantitative results, and on B-scan ultrasound images of a kidney to illustrate its operation.

These algorithms open the way for 3D ultrasound data to be constructed from conventional B-scans using speckle decorrelation, without the requirement to have access to lower level signals from within the ultrasound machine.

Appendix A. Fractional order moments of the exponential distribution

The PDF of the exponential distribution is

$$p(I) = \frac{1}{2\sigma^2}\exp\left(\frac{-I}{2\sigma^2}\right)$$

The nth order moment is therefore

$$\langle I^n\rangle = \int_0^\infty \frac{I^n}{2\sigma^2}\exp\left(\frac{-I}{2\sigma^2}\right)\mathrm{d}I$$

Using Euler's integral from page 255 of Abramowitz and Stegun (1970), we obtain $\langle I^n\rangle = (2\sigma^2)^n\Gamma(n+1) = \langle I\rangle^n\Gamma(n+1)$. Thus the normalised nth order moment of the distribution is given by $\langle I^n\rangle/\langle I\rangle^n = \Gamma(n+1)$.

Appendix B. Homodyned k-distribution

The PDF of the homodyned k-distribution is given by Jakeman and Tough (1987) and Dutt and Greenleaf (1994) as

$$p_A(A) = \frac{1}{\sigma\Gamma(\mu)}\sqrt{\frac{2\mu A}{\pi s}}\sum_{m=0}^{\infty}\left\{\frac{\Gamma(\frac{1}{2}+m)}{m!\Gamma(\frac{1}{2}-m)}\left(\frac{-\sigma^2}{sA\mu}\right)^m \times\left(\frac{|s-A|\sqrt{\mu}}{\sigma\sqrt{2}}\right)^{\mu+m-1/2} \times \mathrm{K}_{\mu+m-1/2}\left(\frac{|s-A|\sqrt{2\mu}}{\sigma}\right)\right\}$$

where s^2 is the coherent backscattered signal energy, $2\sigma^2$ is the diffuse signal energy, μ is the effective number of scatterers per resolution cell (Dutt and Greenleaf, 1995) and $K_n(x)$ is the modified Bessel function of the second kind. The intensity signal I used in the present paper is assumed to be distributed as A^2.

Appendix C. Solving for k and β in terms of R and S

If we take six times Eq. (1) plus Eq. (2) we obtain a quartic equation $3U^4 - (6R+S)U^3 + 6U^2 - 1 = 0$ in $U = \sqrt{k^2+2\beta+1}$. Using symbolic algebra software, the solutions to this equation can be expressed in terms of the following quantities:

$$d = 6R + S$$

$$t = \sqrt[3]{64 - d^2}$$

$$l = \sqrt{d^2 - 48 + 12t}$$

$$m = \sqrt{2d^2 - 96 - 12t + (2d^3 - 144d)/l}$$

$$n = \sqrt{2d^2 - 96 - 12t - (2d^3 - 144d)/l}$$

The four solutions for U are: $U_1 = (d+l+m)/12$, $U_2 = (d+l-m)/12$, $U_3 = (d-l+n)/12$, and $U_4 = (d-l-n)/12$.

From these values of U, we calculate corresponding solutions for k and β, rejecting negative or imaginary values:

$$k = \sqrt{2UR - 2} \qquad \beta = \frac{1}{6}\left(US + \frac{1}{U^2} - 3\right)$$

References

Abramowitz, M., Stegun, I.A., 1970. Handbook of Mathematical Functions. Dover, NY.

Chen, J.-F., Fowlkes, J.B., Carson, P.L., Rubin, J.M., 1997. Determination of scan-plane motion using speckle decorrelation: theoretical considerations and initial test. Int. J. Imag. Syst. Technol. 8, 38–44.

Clifford, L., Fitzgerald, P., James, D., 1993. Non-Rayleigh first-order statistics of ultrasonic backscatter from normal myocardium. Ultrasound Med. Biol. 19 (6), 487–495.

Crawford, D.C., Bell, D.S., Bamber, J.C., 1993. Compensation for the signal processing characterisitics of ultrasound B-mode scanners in adaptive speckle reduction. Ultrasound Med. Biol. 19 (6), 469–485.

Dutt, V., Greenleaf, J.F., 1994. Ultrasound echo envelope analysis using a homodyned *k* distribution signal model. Ultrason. Imag. 16, 265–287.

Dutt, V., Greenleaf, J.F., 1995. Speckle analysis using signal to noise ratios based on fractional order moments. Ultrason. Imag. 17, 251–268.

Dutt, V., Greenleaf, J.F., 1996a. Adaptive speckle reduction filter for log-compressed B-scan images. IEEE Trans. Med. Imag. 15 (6), 802–813.

Dutt, V., Greenleaf, J.F., 1996b. Statistics of the log-compressed echo envelope. J. Acoust. Soc. Am. 99 (6), 3817–3825.

Jakeman, E., Tough, R.J.A., 1987. Generalized *k* distribution: a statistical model for weak scattering. J. Opt. Soc. Am. A 4 (9), 1764–1772.

Kaplan, D., Ma, Q., 1994. On the statistical characteristics of log-compressed Rayleigh signals: theoretical formulation and experimental results. J. Acoust. Soc. Am. 95 (3), 1396–1400.

Li, M., 1995. System and method for 3D medical imaging using 2D scan data. United States patent 5,582,173. Application number 529778.

Ossant, F., Patat, F., Lebertre, M., Teriierooiterai, M.-L., Pourcelot, L., 1998. Effective density estimators based on the *k* distribution: interest of low and fractional order moments. Ultrason. Imag. 20, 243–259.

Smith, W.L., Fenster, A., February 2000. Optimization of 3D ultrasound scan spacing using speckle statistics. In: Shung, K.K., Insana, M.F. (Eds.), Ultrasonic Imaging and Signal Processing, Proc. SPIE, Vol. 3982. San Diego, California.

Tuthill, T.A., Krücker, J.F., Fowlkes, J.B., Carson, P.L., 1998. Automated three-dimensional US frame positioning computed from elevational speckle decorrelation. Radiology 209, 575–582.

Wagner, R.F., Smith, S.W., Sandrik, J.M., Lopez, H., 1983. Statistics of speckle in ultrasound B-scans. IEEE Trans. Son. Ultrason. 30 (3), 156–163.

Weng, L., Reid, J.M., Shankar, P.M., Soetanto, K., 1991. Ultrasound speckle analysis based on the *k* distribution. J. Acoust. Soc. Am. 89 (6), 2992–2995.